APPLICATION OF A HEAT BARRIER SLEEVE TO PREVENT SYNCHRONOUS ROTOR INSTABILITY

by

Frits M. de Jongh

Research and Development Engineer

and

Pieter van der Hoeven

Manager, Test Engineering

Demag Delaval Turbomachinery

Delaval Stork V.o.f.

Hengelo, The Netherlands

Frits M. de Jongh is a Senior Research and Development Engineer for Demag Delaval Turbomachinery at Delaval Stork V.o.f., Hengelo, The Netherlands. He has more than 15 years of diversified experience in the fields of testing rotating machinery, solving vibration problems, rotordynamic research, and compressor stage performance investigations. He joined the company's R&D department in 1989, where he is currently responsible for the development of design and analysis methods in the area of applied mechanics, and dynamics of rotating machinery.

Mr. de Jongh received a B.Sc. degree (Mechanical Engineering) from the Dordrecht Institute of Technology (1980), and also has a B.Sc. degree in Economical Industrial Technology. He has authored and coauthored several technical turbomachinery papers.

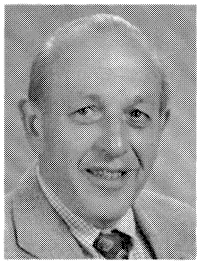

Pieter van der Hoeven is Manager, Test Engineering for Demag Delaval Turbomachinery at Delaval Stork V.o.f., in Hengelo, The Netherlands. He worked eight years for Shell as a Merchant Marine Engineer. Since joining the Stork company, he has worked six years on projects involving commissioning, testing, and extensive troubleshooting at thermal and nuclear power plants. He has had several assignments in various disciplines, including testing of high pressure compressor units with natural gas in accordance with ASME/PTC-10 Class I. Currently, Mr. van der Hoeven is responsible for all aspects related to the testing of high speed rotating machinery.

Mr. van der Hoeven graduated from the Rotterdam Institute of Technology (1965) with a B.Sc. degree in Mechanical Engineering.

ABSTRACT

This paper explains how synchronous rotor instability can occur in high speed turbomachinery due to differential heating of bearing journals. Theoretical investigations have indicated that rotors supported by fluid-film bearings inherently exhibit a nonuniform temperature distribution around the bearing journal circumference (Keogh and Morton, 1993, 1994). This thermal effect results in rotor bending, which in combination with an overhung mass, such as couplings and overhung impellers, can significantly increase rotor unbalance and thus, synchronous rotor vibration. Under certain conditions, it can even lead to synchronous rotor instability. In this paper, a case history on synchronous rotor instability is presented, concerning two pipeline compressors for a natural gas application. The compressors successfully passed an API 617 mechanical running test in the manufacturer's workshop. However, installed at site, the rotor behavior of these machines was completely unstable. The vibration analysis indicated that the cause of the instability was likely to be thermal in origin. However, ordinary labyrinth seal rubbing could be excluded. One of the compressor cartridges was returned to the manufacturer's workshop for a detailed examination and an extensive test program. It appeared that rotor instability was caused by differential heating of the impeller-end bearing journal, which could not be reduced by modification of the bearing parameters. Eventually, a *heat barrier sleeve* was designed to prevent thermal bending of the rotor at this location. Additional testing confirmed the expected effect and, after installation in the field, the unstable behavior of both machines was completely eliminated.

INTRODUCTION

Synchronous rotor instability due to bearing journal differential heating is not a well known rotordynamic phenomenon. One of the reasons is that synchronous instability is probably not recognized as such. On the other hand, if it is considered as a possible cause, it will be difficult, or impossible in most cases, to measure differential temperatures in a rotating shaft to identify the cause of the vibrations. The phenomenon has been extensively investigated on a particular compressor rotor at the authors' company and results were published by de Jongh and Morton (1996). A simplified description of the phenomenon is given in APPENDIX A, and an experimental verification is given in APPENDIX B.

The case history described in this paper is an example of a vibration problem caused by bearing differential heating. During commissioning of two identical centrifugal compressors, unexpected synchronous rotor vibrations were observed on both units. The compressors were applied in a Dutch gas station for the transportation of natural gas, each compressor directly driven by a 10,000 kW gas turbine. Figure 1 shows a cross section of the compressor. The operating speed range was defined as 5,370 rpm to 9,400 rpm (maximum continuous speed). The design flow is 30,500 m^3/hr at suction conditions of 54 bars at 7°C, and the discharge conditions are 64 bars at 21°C. The total rotor mass is around 265 kg, and the rotor is supported by two fluid-film, tilting-pad type journal bearings and a tilting-pad type axial bearing. Figure 2 shows the undamped critical speed map for the rotor bearing system and, in Figure 3, the corresponding modeshapes are given. A tandem dry gas seal is used to seal the machine behind the overhung impeller. Inboard of each bearing, two noncontacting

eddy-current displacement probes were located in one plane, spaced 90 degrees apart.

In the design stage, a routine check on the sensitivity for synchronous rotor instability was performed for these machines, and, as a result of this analysis, the width of the journal bearing at the impeller end was reduced. The analysis further showed that 10 percent variation of the impeller overhung weight had minor influence on the results. Prior to shipment, both compressors were successfully subjected to an ASME/PTC-10 Class III test (ASME, 1965) in the manufacturer's workshop. These tests were executed at a running speed of 8,850 rpm with air in an open loop arrangement. Also on both units in the same open loop, a mechanical running test according to API 617 (API, 1979) was performed. Tests were carried out up to trip speed (9,870 rpm). During these tests, the compressor was driven via a shop gear by a variable speed electric motor. Since the gas turbine contract coupling was not available at that time, a test stand coupling with the same overhung moment was used. The compressors successfully passed all the required testing criteria, and the units were shipped to site.

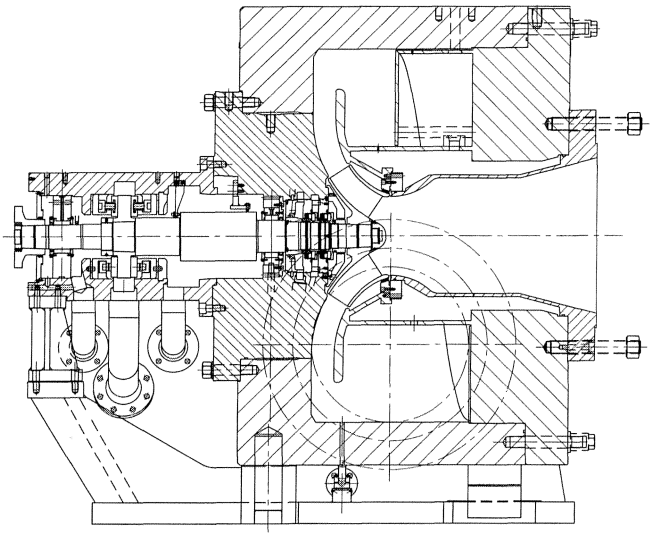

Figure 1. Longitudinal Section of Centrifugal Compressor.

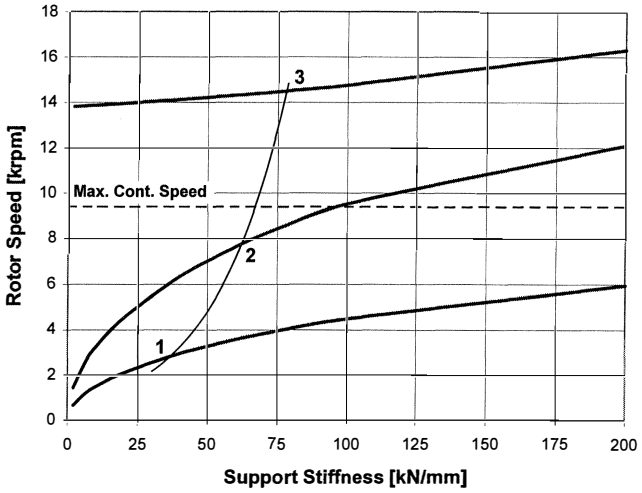

Figure 2. Undamped Critical Speed Map.

PROBLEM DESCRIPTION

During commissioning at site, unexpected vibration problems were encountered on both units. The first running tests, up to

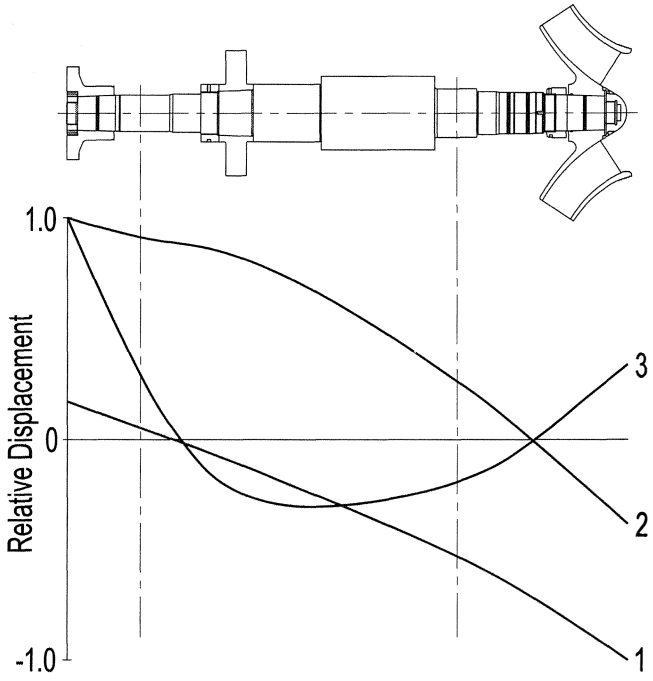

Figure 3. Rotor Configuration with Undamped Critical Speed Modeshapes.

7,200 rpm (76 percent of maximum continuous speed), were satisfactory with maximum vibration levels of around 12 microns peak-to-peak (0.5 mil). Above 7,200 rpm however, the rotor vibration behavior was unacceptable, and both compressors were tripped several times on high vibration. At these higher speeds, the vibration levels were normal, until a sudden increase in vibration levels tripped the unit at a level of 75 microns peak-to-peak (3 mil). The vibration analysis showed that the predominant frequency of all signals was synchronous with running speed. Figure 4 shows a typical plot of the rotor vibration behavior, measured at the impeller-end bearing. For one of the runups, Figures 5 and 6, respectively, give the rotor speed and the vibration level as a function of time. For this run, above a certain speed the vibrations were varying between a minimum and a maximum value, although the rotor speed was constant. Figure 7 shows a polar plot of this run at a rotor speed of around 8,400 rpm.

The time involved from low vibrations to trip level depended on the rotor speed and varied from about one to two minutes. Sometimes it was possible to continue running for a period of a few hours; however, at other times, the phenomenon occurred three times in one hour. A practical remedy was employed by raising the speed extremely slowly. If any signs of increasing vibration levels were noticed, the speed was immediately reduced by 500 rpm. By doing this, one of the units only had a trip on high vibrations after eight hours. We believed that if the unit was not tripped, the vibration levels would have become extremely high.

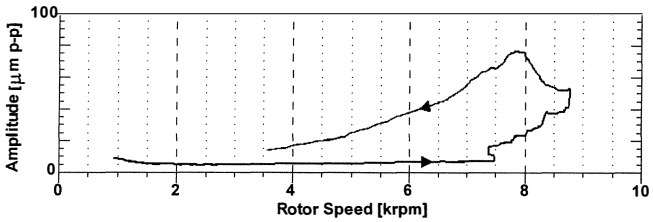

Figure 4. Fundamental Component (1×) of Relative Shaft Vibration, Measured at Impeller-End Bearing.

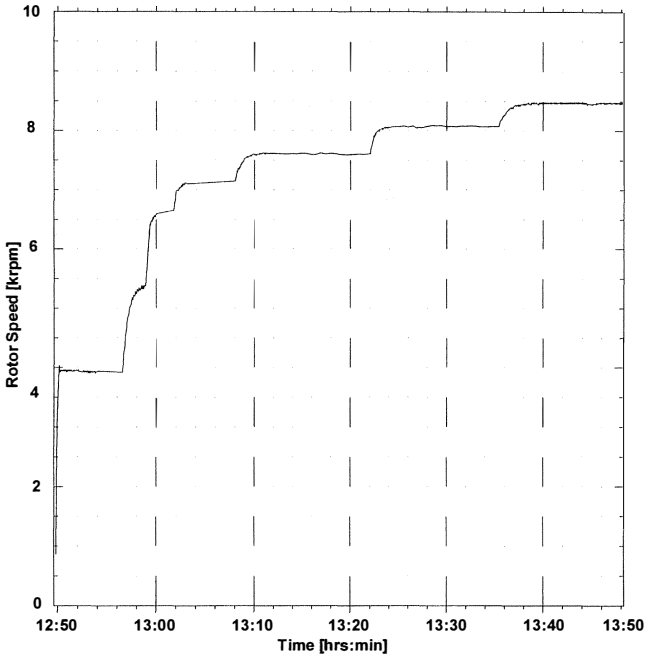

Figure 5. Rotor Speed Versus Time.

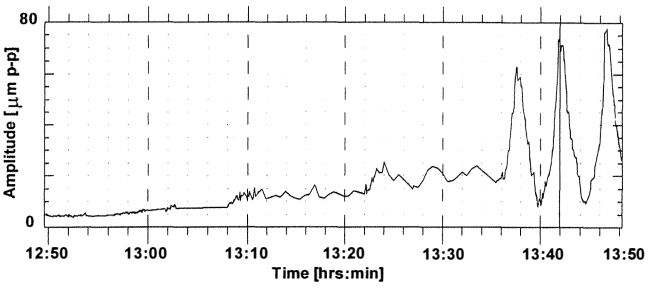

Figure 6. Unfiltered Relative Shaft Vibration Versus Time, Measured at Impeller-End Bearing.

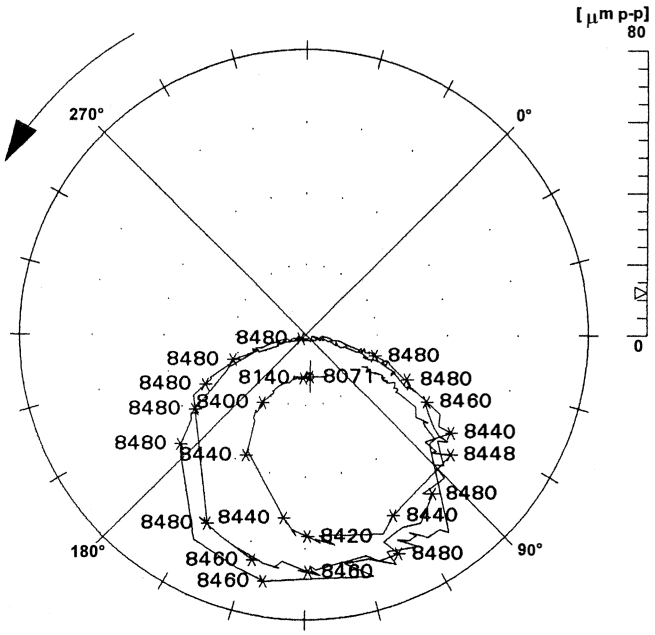

Figure 7. Filtered Shaft Vibration (1×) at a Constant Speed.

Although the vibrations were synchronous with running speed (1×), it was not possible to field balance the rotor. The phase change in Figure 7 shows a continuously changing unbalance vector. Finally, the compressor suction and discharge piping were removed, and, in this configuration, another test run was conducted. This test run, with open suction and discharge piping (air test), was executed with all other contract equipment in place. During this test, the vibration levels were low over the entire speed range and stayed low, no matter what was done. Quick starting or stopping procedures, changing oil supply temperatures, fast rotor speed changes—nothing changed the low vibrations. In fact, the running behavior was similar as to what was experienced in the manufacturer's workshop.

PROBLEM APPROACH

Resuming the vibration problem, the compressor had high synchronous rotor vibrations, which could not be predicted by the traditional rotordynamic analyses. The undamped critical speed map in Figure 2 indicates that, to reach maximum continuous speed, two critical speeds have to be passed. As can be seen in Figure 3, these critical speeds have typical conical rigid body modeshapes. Rotor response calculations showed that these modes are both critically damped (AF less than 2.5). The next critical, above the operating speed range, is the first bending mode, which has an amplification factor of around five, and the separation margin to the maximum operating speed is sufficient.

The rotor vibration behavior was not stable, but was changing in time. The vibrations sometimes were varying between a minimum and a maximum value, although the rotor speed was constant. It was noticed that, during this unstable behavior, the phase angle was also changing continuously. The high vibrations could be suppressed by reducing the rotor speed, but hysteresis was shown in the plots between the runup and coastdown. It can be seen in Figure 4 that during reducing the rotor speed, the vibration level was much higher than during the runup. This hysteresis points into the direction of a thermal phenomenon. However, without the suction and discharge piping connected to the compressor, the machine ran well.

Figures 6 and 7 could also indicate a severe rub between rotor and static parts, such as labyrinths. In that case, the mechanical contact produces a hot spot on the shaft, which results in a thermal bend. The varying vibration levels and corresponding phase changes would be the result of a combined action of the rotor unbalance and the continuously changing unbalance from the thermal bend. This effect is often referred to as the "Newkirk effect" (Newkirk, 1926) or also as "spiral vibrations," due to its nature. That the generation of spiral vibrations can also be caused by stationary elements other than labyrinths, was described by Kellenberger (1979) and also by Schmied (1987).

It has to be mentioned that some high piping forces were expected in the design phase, and for this reason the compressor casing had been made very stiff. The actual piping forces, however, were checked and appeared to be relatively low. For this reason, casing distortion and, thus, consequent shaft rubbing as the cause for the vibration problem, was ruled out.

Figures 6 and 7, in themselves, could be an example of synchronous rotor instability; a phenomenon in which a thermal bend develops at one of the bearing journals, and in combination with a free overhang moment, generates synchronous unstable vibrations. This phenomenon was observed by the authors during the past few years on various types of turbomachinery such as compressors, expanders, gas turbines, and gears. Experimental work at the authors' company on several test rotors confirmed significant differential temperatures across the bearing journals, leading to the assumption that differential heating of bearing journals, in practice, occurs on all rotors supported by fluid-film bearings. Based on these experimental investigations and an analytical model, a calculation program was developed to predict the onset of synchronous rotor

instability for new applications. The principle of this program is described in APPENDIX C. However, the design check performed on this compressor and all the running tests carried out on air, including the test in the field without suction and discharge piping, seemed to preclude synchronous rotor instability.

For maintenance purposes, all significant parts of the compressor are combined in a "cartridge," as can be seen in Figure 8. This cartridge was sent back to the supplier's works for a detailed inspection of all parts, but nothing unusual was found that could explain the cause of the vibration problem. There were no significant rubbing marks on the shaft, the hydraulic shrink fits of the impeller and the coupling hub were correct, and there was a proper fixture of the rotating seal part to the rotor. The bearings were both in a perfect condition and the diametrical clearances of 0.195 percent at the driven-end (DE) and 0.19 percent at the nondriven-end (NDE) were found within the specifications. The dry gas seal was also in a perfect condition. The only interesting part was the impeller-eye labyrinth where, due to rubbing, the diametrical clearance was increased to about 1.1 mm. However, if this labyrinth is the cause of the problem, then Figures 6 and 7 cannot be explained since this labyrinth is at the very end of the rotor and not even directly positioned on the shaft. The damage to this labyrinth was defined as the result of high rotor vibrations and not as the root cause of the problem.

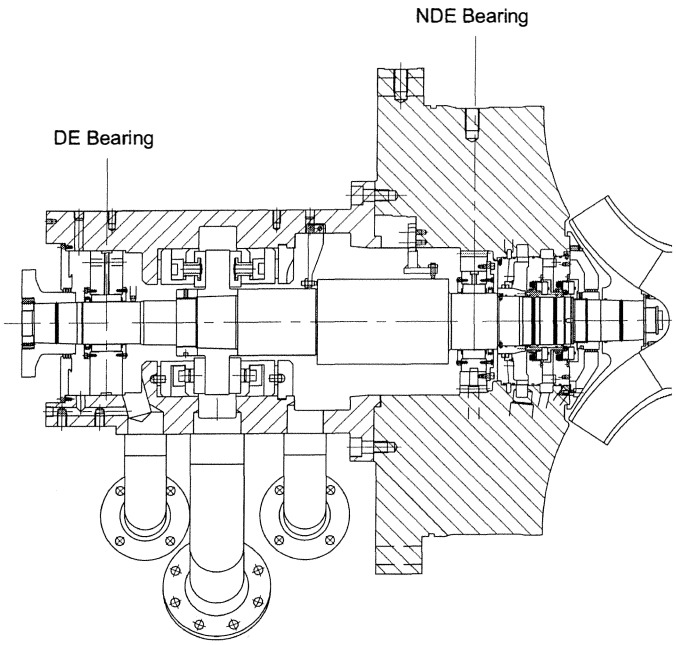

Figure 8. Longitudinal Section of Compressor Cartridge.

By then, it was decided to handle the cartridge as a real compressor. It was installed on the test bed floor and driven, via the contract coupling and a shop gear, by a shop variable speed electric motor. As with all other tests carried out with air, the vibrations were low and stable over the full operating speed range. After this test, the impeller was removed and changed out for a "dummy" impeller, a disk with the same shrink fit to the shaft and the same dynamic characteristics and total weight as the actual impeller. However, the dummy impeller weight could be reduced by 10 kg by removing a ring. By adding another ring, a 10 kg heavier impeller could be simulated. Figure 9 shows this test setup. Also, a dummy impeller check nut, suitable for mounting noncontacting vibration probes, was installed at the location of the impeller nose cone. To establish the rotor mode shape during testing, additional pairs of noncontacting vibration probes were installed at the coupling hub, at midspan between the bearings, and on the impeller check nut.

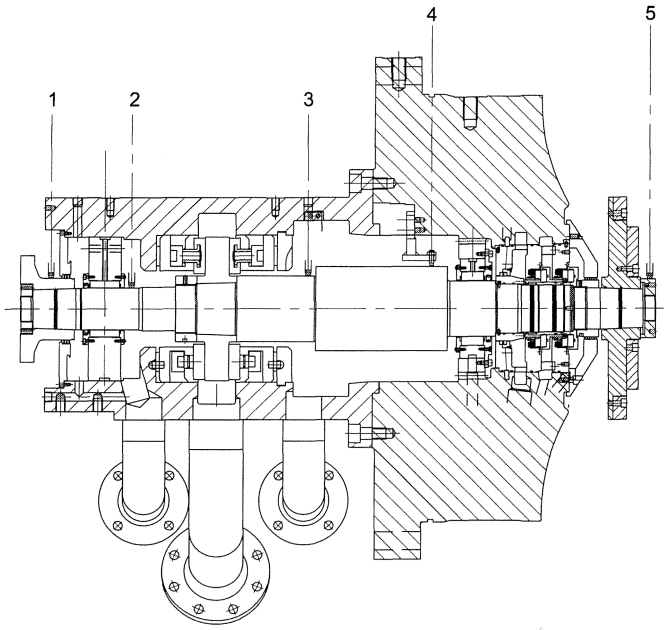

Figure 9. Compressor Cartridge with Dummy Impeller for Testing Purposes.

In this configuration, it was relatively easy to change several parameters and test their influence, such as running without the impeller, with various impeller weights, with and without the dry gas seal, with and without unbalance, with the bearing load on pads or between pads. However, whatever we did, the vibrations stayed low and stable in all configurations over the complete operating speed range.

As starting was becoming a kind of routine, the first start on day four to full speed was executed within two minutes, which was much faster than the days before. At this point, synchronous vibrations started to rise, and around one minute later the unit was tripped on one of the job vibration probes close to the impeller-end bearing, at a vibration level of 75 microns peak-to-peak. Whatever was done during the rest of the day, the vibration levels stayed low and stable over the whole speed range. During the first quick startup the next morning, the unstable rotor behavior was repeated. All other test runs during that day were stable again.

INTERIM CONCLUSION

As can be seen in Figure 8, the cartridge consists of a relatively large steel part around the impeller-end bearing (NDE). On the test bed, during the first start in the morning, the metal is cold with a temperature of around 14°C. During the quick start, the bearing is heated, but restricted in thermal expansion and, as a consequence, the bearing pads will grow inward and the clearance will be slightly reduced. During all other tests of the same day, due to the heat produced by the bearing and the dry gas seal, the temperature of this steel part was increasing to around 45°C and the bearing operating clearance was "normal." As the process gas, being gas from a pipeline with a temperature of around 5°C, has a very high cooling effect on this steel part during compressor operation with process gas, the bearing clearance is expected to stay slightly reduced. A recalculation for synchronous rotor instability, with a reduced NDE bearing clearance, showed a significant reduction for the stability margin. To verify this interim conclusion, it was decided to reduce the bearing clearance of the NDE bearing from 0.19 to 0.16 percent. During the following tests, the rotor vibration behavior was similar as observed at site. Above 8,000 rpm, at randomly selected speeds, the rotor started to become unstable and within one or two minutes the vibration trip levels were reached. The test was repeated without the dry gas seal and without any

labyrinths installed. In this case, the only possible "contact" with the rotor were the bearings. The unstable rotor behavior at site could be reproduced completely, and also during these test runs it was sometimes possible to continue running, if speed changes were made very slowly. But a speed increase of 1,000 rpm within 10 seconds directly triggered the instability. Only small variations in vibration behavior were found when running with a lighter or heavier impeller wheel. One of these test runs is shown in Figures 10, 11, and 12. These plots also show cyclic variation in amplitude and phase, as seen at site (Figures 5, 6, and 7), and also a significant hysteresis was found between runup and coastdown vibration levels as seen in Figure 4. From the rotor modeshapes in Figure 3, it can be seen that for the second mode there is a node between the NDE bearing and the impeller. Rotor response calculations with a single unbalance at the impeller showed that, in the region of this mode, the response at the bearing location was around 180 degrees out-of-phase with the impeller unbalance. For synchronous rotor instability, this condition is necessary for a thermal bow to increase. Depending on the rotor speed, the phase angle will be slightly different from 180 degrees. This means that for each speed, the mentioned phase relationship results in a hot spot that is gradually moving around the journal circumference. This thermal effect results in a continuously changing unbalance vector, or cyclic vibrations in the time domain, which was observed for this machine. It was concluded without any doubt: the observed rotor behavior was synchronous rotor instability.

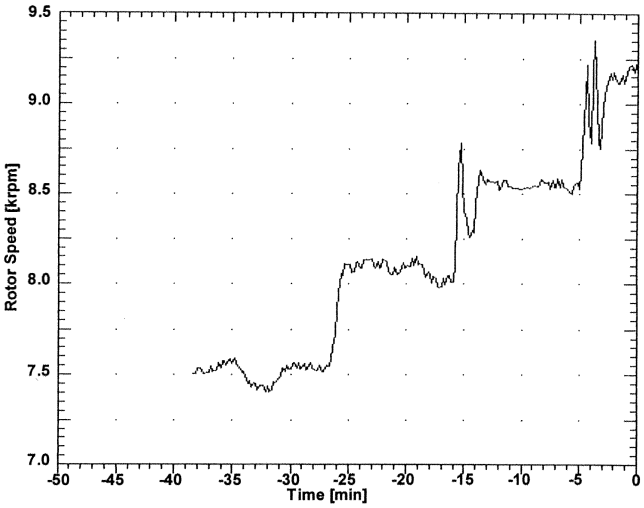

Figure 10. Rotor Speed Versus Time.

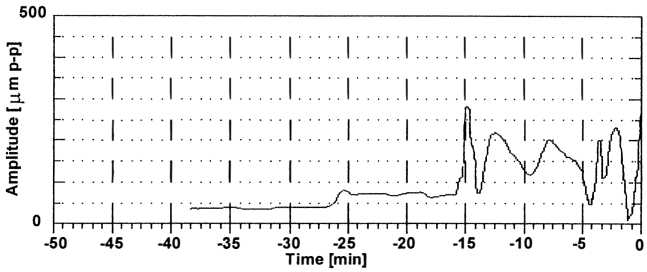

Figure 11. Filtered Shaft Vibration (1×), Measured at the Dummy Impeller Check Nut.

SOLUTION

Considering all the results described above, a simple solution was possible. If the compressor is operating on natural gas at a temperature of around 5°C, then make sure that the operating bearing clearance is kept above a certain threshold value. In practice, an increase of the cold bearing clearance of the NDE

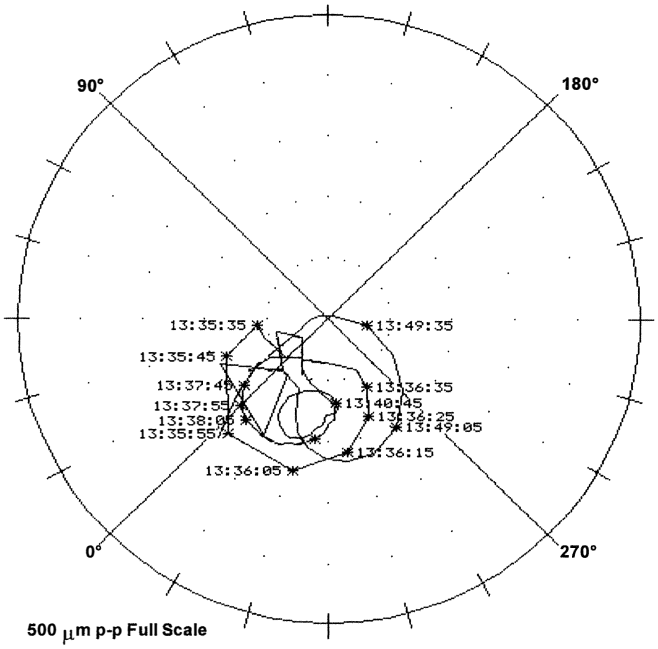

Figure 12. Filtered Shaft Vibration (1×), Measured at the Dummy Impeller Check Nut.

bearing to 0.22 percent should solve the problem. However in that case, the small difference of 0.03 percent in bearing clearance is the difference between a good running compressor or a completely unacceptable machine. For this reason, it was felt that this was not an acceptable solution. The root cause of the problem was defined as the differential temperature across the shaft, generated by differential shearing in the oil-film, as explained in APPENDIX A. However, the generated differential heating at the bearing journal cannot be eliminated, since it is inherent to the journal behavior in the fluid-film bearing. It was argued if it would be possible to reduce the consequent thermal bending of the shaft. With this in mind, the heat barrier sleeve was developed and a typical design is shown in Figure 13. The actual heat barrier, which greatly reduces the differential heat flow to the shaft, is the gap created between the sleeve and the shaft. In Figures 14 and 15, an example is given of a typical temperature distribution across the shaft without and with the sleeve, respectively. Since analytical calculations were promising a significant reduction of the shaft differential temperature, it was decided to design and build the heat barrier sleeve. Various materials were discussed for the sleeve, but finally for this application, it was decided to use the same material as the shaft and leave the gap filled with air. To check the mechanical behavior of the sleeve, a finite element stress analysis was carried out.

With great care, to prevent any additional changes, the unstable compressor cartridge was disassembled and inspected, and a runout protocol of the shaft was made. Comparison with the initial measurements did not show any changes. Since it was the intention to apply the sleeve for the existing bearing, the shaft diameter had to be reduced. Calculations showed that this diameter reduction hardly changed the rotordynamic characteristics of the rotor. Final machining was done by grinding, keeping the diameter concentric with a reference diameter. After a check on the shaft runout, the sleeve was mounted on the shaft with a shrink fit. Using the same reference diameter, the sleeve was ground to the final dimensions, within 0.005 mm (TIR) of the original shaft dimensions. The final protocol of the shaft showed that the shrinkage of the sleeve did not affect the rotor runout.

EXPERIMENTAL RESULTS

After mounting the heat barrier sleeve on the shaft, a successful unbalance check was performed. The compressor cartridge was

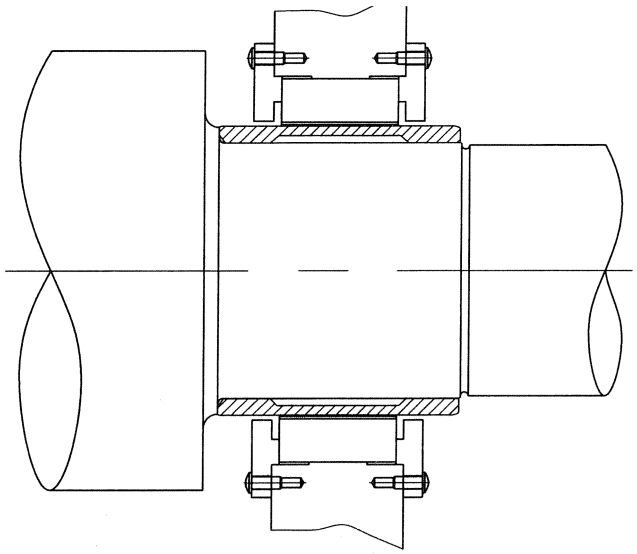

Figure 13. Typical Heat Barrier Sleeve.

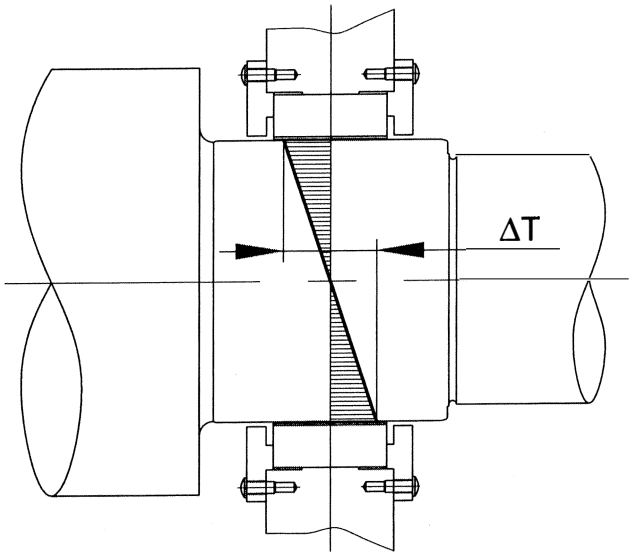

Figure 14. Typical Temperature Distribution Across Bearing Journal.

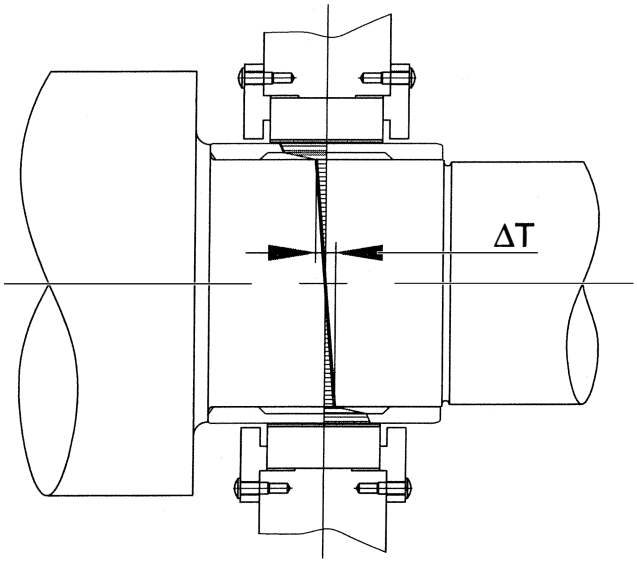

Figure 15. Typical Temperature Distribution with Heat Barrier Sleeve.

assembled as before, and test runs were started. The compressor rotor behavior was perfect in all aspects, over the entire operating speed range, with low vibrations. No signs of instability were found. Smaller and larger bearing clearances were tested, but the rotor behavior was no longer sensitive to any clearance changes. Tests with different overhung weights were carried out again. Finally, the dummy impeller wheel was replaced by the original impeller and a last check run was executed. To review, the rotor vibrations were low and completely stable. Shortly thereafter, the compressor was shipped to site and was tested over the entire speed range with all kinds of gas flows and pressures, and the vibrations remained low and stable. As can be seen in Figure 16 the vibration level was less than 25 microns peak-to-peak (1 mil). The application of the heat barrier sleeve completely eliminated the vibration problem. A similar heat barrier sleeve was fitted on the rotor of the second compressor, and the running behavior at site was also completely stable.

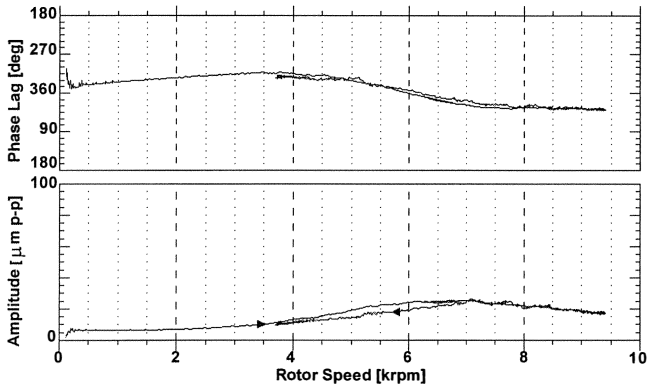

Figure 16. Fundamental Component (1×) of Relative Shaft Vibration, Measured at Impeller-End Bearing (with Heat Barrier Sleeve).

DISCUSSION

The authors assume that a few percent of newly designed equipment is practically affected by this phenomenon, especially for high speed turbomachinery with relatively high overhang moments. Not only overhung compressors or expanders, but also drive-through machines with couplings at both overhung ends of the rotor. The phenomenon was recently observed by the authors on the high speed pinion of a parallel shaft gearbox. This gear was successfully tested according to the API 613 Standard (API, 1988), although the coupling half-weight simulator was not applied. When coupled to a compressor with the quite heavy contract coupling for a no-load string test, high unstable synchronous vibrations were encountered at the gear pinion. Investigations at the test stand and a calculation check with the program described in APPENDIX C, confirmed synchronous rotor instability. The calculation program predicted that an overhung weight reduction of around 5 kg was just sufficient to shift the onset of the instability above operating speed, and this was confirmed at the test stand. The final coupling overhung weight could be reduced by 9 kg, and further testing confirmed that the vibration problem was completely solved.

Faulkner, et al. (1997), describe a case history of a radial inflow overhung turbine exhibiting the described phenomenon. The problem was recognized and solved by changing the bearing geometry. It was argued that the thermal bowing would be less effective if the bearing would be loaded to a higher eccentricity. Further experimental investigations were executed at the authors' company to establish the influence of various bearing parameters on the thermal effect, among which were the specific bearing load. A special bearing test rig has been developed for this purpose.

Corcoran, et al. (1997), describe a very interesting and extensive case history on a compressor rotor with a high coupling overhung

moment. We suppose that this paper describes a typical synchronous rotor instability problem at the coupling-end bearing, although it was not mentioned. It is interesting to see that the problem could be solved either by decreasing or significantly *increasing* the coupling weight. The theory confirms that under certain circumstances, also the latter solution is possible.

Stroh, et al. (1996), mention that for overhung rotors, there is a difference in balance condition when balancing an impeller on a mandrel between two bearings or with the impeller mounted on the overhung. In the latter case, the rotor is more sensitive. They say that the reason for this is unclear. It might be that the subject of our paper provides the answer.

Since 1992, when the described phenomenon was known by the authors, a calculation method was developed to check newly designed rotating equipment for possible synchronous rotor instability (APPENDIX C). If synchronous instability is expected in the design stage, the following corrective actions can be considered:

- Limit the design speed.
- Reduce overhang moments.
- Increase or decrease bearing clearances.
- Reduce bearing width.
- Change bearing geometry.
- Apply heat barrier sleeve (for which the authors' company has applied for a patent).

In the design stage, usually several changes are possible. It is advised to first optimize the rotor on response at the bearing location, due to unbalance at the overhung. If not enough margin can be obtained, then the application of a heat barrier sleeve can be considered. Also, for machines in operation with a history of marginal synchronous vibration behavior, a heat barrier sleeve might be an alternative.

CONCLUSIONS

A synchronous rotor instability problem was encountered on two identical overhung compressors when commissioned at site. The compressors successfully passed an API 617 mechanical running test in the manufacturer's workshop prior to shipment. Additional testing of the compressor cartridge showed that differential heating of the bearing journals was the root cause of the unstable rotor behavior. The NDE bearing operating clearance at site appeared to be smaller, as during shop testing. The application of a heat barrier sleeve completely eliminated the vibration problem on both units.

There seems to be no recognition in the rotordynamic literature (apart from references listed in this paper) of the possibility of differential journal heating resulting in problems of synchronous vibration, either in terms of sensitivity or instability. Where such problems have occurred, they have often been resolved pragmatically by changing overhang moments or altering bearing geometry. A bearing test rig developed in the authors' company is currently being used to investigate the effect of bearing design and operating parameters on the differential journal heating effect. Also, further work is being carried out to optimize the heat barrier sleeve.

The authors believe that knowledge of the described differential heating phenomenon will contribute to a better understanding of rotordynamic behavior of high speed turbomachinery.

NOMENCLATURE

G = Gain vector
I = Influence coefficient
M_c = Concentrated overhung mass
R = Radius
T = Thermal gain
U = Unbalance
h = Distance between journal and bearing wall
l = Overhang length
t = Time
v = Velocity
ϵ = Orbit vector
φ = Phase angle
θ = Change in shaft slope at bearing journal
Ω = Rotational speed

Subscripts:

i = Input
o = Output
O = Overhang position
B = Bearing position

APPENDIX A

The Phenomenon of Synchronous Rotor Instability

This appendix gives an explanation of bearing journal differential heating, which is the root cause of synchronous rotor instability. This type of thermal rotor instability is caused by a temperature effect that appears in all practical fluid-film bearings. The nature of the instability is synchronous with the rotor speed. In the traditional bearing literature, it is normally assumed that a rotating bearing journal has a uniform temperature distribution around the journal circumference. However, this assumption does not hold true when a journal is orbiting in its bearing with a whirl frequency synchronous to the rotor speed (Morton, 1994). In fact, every journal will execute a small synchronous orbit due to residual unbalance in the rotor. Any journal that is synchronously orbiting in a fluid-film bearing produces a temperature difference across its diameter. Figure A-1 shows a bearing journal that is rotating at constant speed, executing a forward circular orbit. One specific point on the journal will always be at the outside of the orbit (the high spot) and will therefore be nearest to the bearing wall. The point opposite of it will always be furthest away from it. At the hot spot in Figure A-1, the distance from the shaft to the bearing wall is always smaller than at the indicated cold spot opposite to it. Since the friction losses are proportional to the velocity gradient in the oil-film, this means that the heat input, due to these friction losses, will not be uniform around the journal circumference. Heat conduction across the journal due to this differential heat input, produces a differential temperature locally across the journal. This will result in a thermal bend. The greater the size of the orbit, the larger the differential temperature. Figure A-1 shows a forward circular orbit, but the same principle applies for a backward orbit when the journal is positioned eccentric in the bearing, although the heat input will be smaller in this case. Since a linear system is assumed, the forward and backward thermal effects can be superimposed for an elliptical orbit.

Figure A-2 shows the thermal instability principle for a rotor with one overhung end. One can imagine for simplicity that the overhung mass, M_c, is concentrated at the rotor end, at a length, l, from the bearing. If we consider for this rotor a very small synchronous orbit vector, ϵ, at the bearing location, a small thermal bend, θ, will be developed due to the differential heating, and the unbalance, $U = M_c\ l \sin(\theta)$, will result at the overhang. The unbalance vector produces a new orbit vector at the bearing location and so on. If the resulting orbit is smaller, the process will decay, but if the resulting orbit is greater, this continuous process will grow. In that case, the system is unstable and the synchronous vibrations increase. Figure A-3 shows the instability scheme, here starting with a small thermal bend, θ_i.

APPENDIX B

Experimental Verification of Bearing Journal Differential Heating

This appendix describes an experimental verification of the theory that bearing journals of fluid-film bearings do not have a

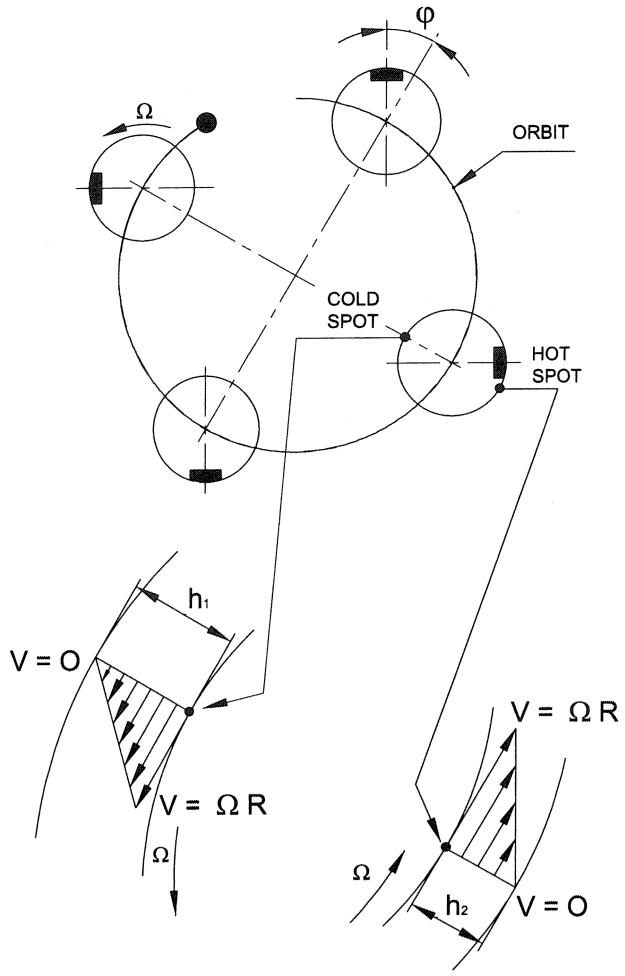

Figure A-1. Differential Heating at Bearing Journal for Synchronous Forward Rotor Whirl.

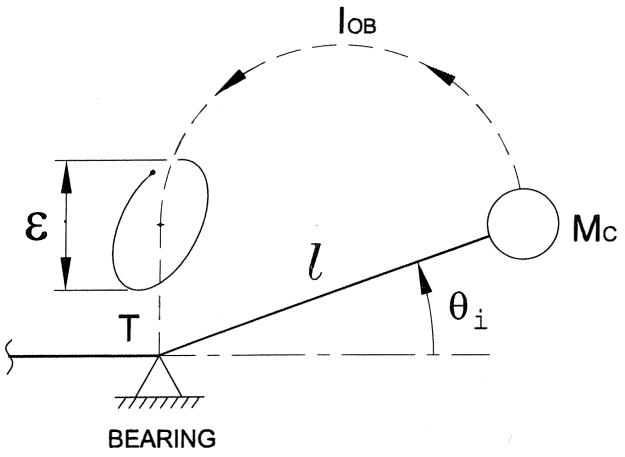

Figure A-2. Thermal Rotor Bend at Bearing.

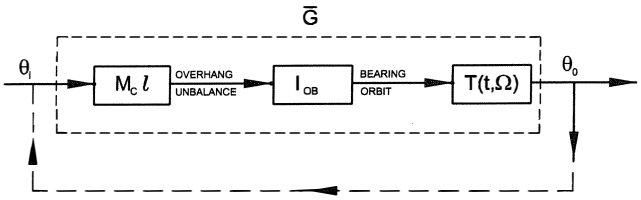

Figure A-3. Scheme of Synchronous Instability Phenomenon.

uniform temperature distribution around the journal circumference, but that a nonuniform temperature distribution exists. The experiment was executed in 1992, in preparation of another rotordynamic R&D project already mentioned (de Jongh and Morton, 1996). A simple test rotor, as shown in Figure B-1 was manufactured. The rotor was supported by two four inch tilting-pad journal bearings. In one of the bearing journals (NDE), four calibrated temperature sensors were installed at 1.0 mm below the journal surface and spaced 90 degrees. Since, according to the theory, the temperature distribution around the journal is sinusoidal, at least four temperature sensors were required to establish the direction and magnitude of any differential temperature across the journal. For the instrumentation used to read out the temperature measurements, see the reference mentioned above. The rotor was driven by a variable speed electric motor in the manufacturer's high speed balancing facility. To transfer the electrical signals from the rotating shaft, a special slipringless transmitter was applied. A photograph of the rotor including the used instrumentation is shown in Figure B-2. The shaft was accurately balanced according to ISO 1940, G = 1.0. During the runup of the shaft, the temperatures increased and when speed was kept constant at 12,500 rpm, they stabilized. Figure B-3 shows a cross section of the shaft at the center of the bearing with the four temperature sensors. The measured temperatures for the first runup, which are nearly equal, are given in Figure B-3(a). The orbit size at the NDE bearing was obtained with two displacement probes, spaced 90 degrees, and after subtraction of the slow roll vector, only around 2 microns peak-to-peak were measured at this speed. The objective of the experiment was to generate a shaft orbit in the NDE bearing and measure the temperature distribution around the bearing journal. To generate a distinct shaft orbit in the bearing, an unbalance weight was applied on the shaft at a defined location at zero degrees. Figure B-3(b) shows the four measured temperatures caused by this shaft orbit. After removing the weight, the temperature values shown in Figure B-3(c) were reproduced within 0.3°C. Figure B-3(c) shows the measured temperatures of the next runup where the unbalance was applied at the same axial location on the shaft, but now rotated over 180 degrees. As can be seen, the direction of the differential temperature was also rotated over about 180 degrees. Further experiments were conducted to obtain a better knowledge of the phenomenon, but are not described in this paper.

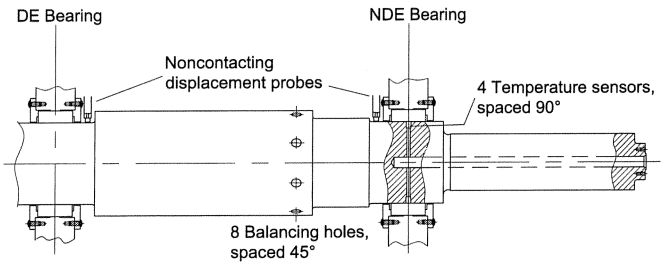

Figure B-1. Test Rotor with Four Temperature Sensors at the NDE Bearing.

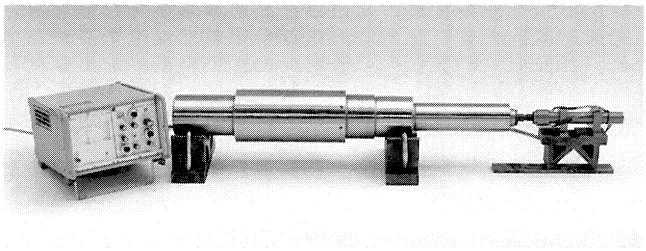

Figure B-2. Test Rotor with Measuring Equipment.

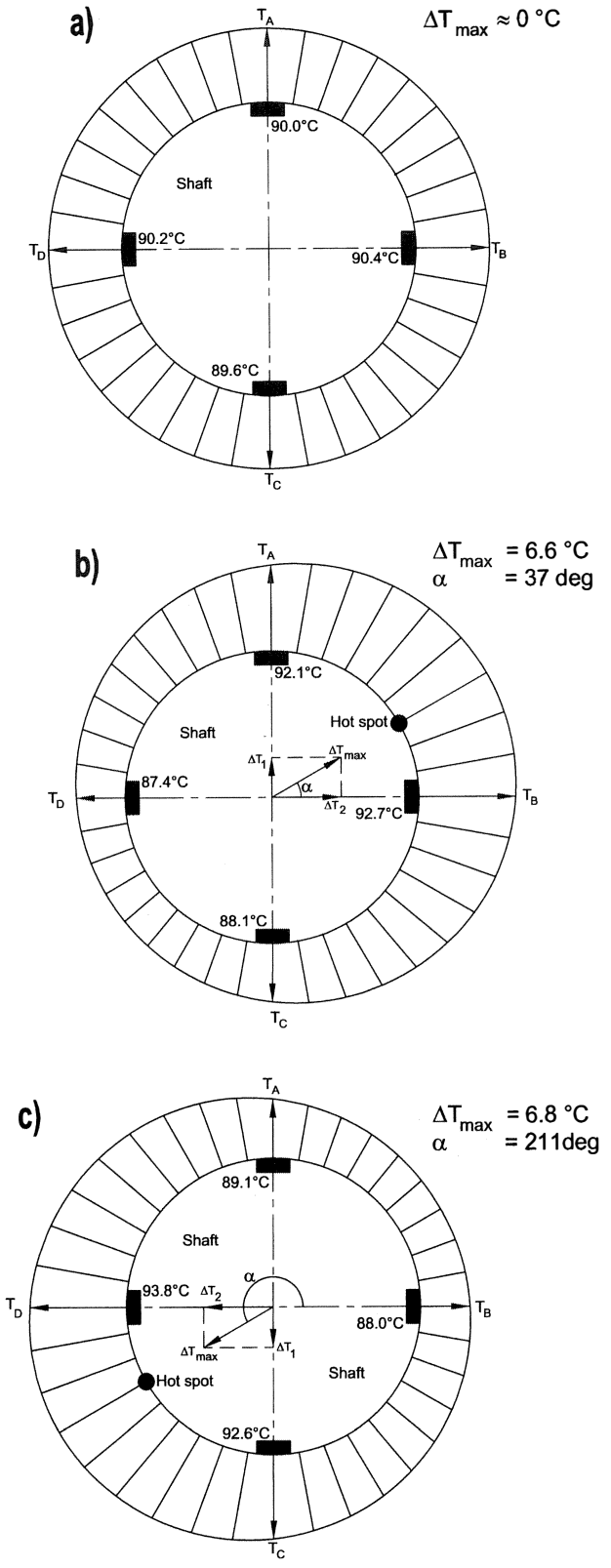

Figure B-3. Cross Section of NDE Bearing Journal, with (Sinusoidal) Temperature Distribution.

APPENDIX C

Prediction of Synchronous Rotor Instability

This appendix describes the principle of a computer program, which was developed to predict the onset of synchronous rotor instability. Referring to Figure A-3, three transfer functions, $M_c \times l$, I_{OB}, and T(t, Ω), are shown for one overhang end of the rotor.

Where:
For a practical rotor, $M_c \times l$ is defined by the overhang geometry (the sum of the distributed overhang moments).
I_{OB} is the complex rotor response between the overhang and bearing locations.
T(t, Ω) is the complex thermal gain and is dependent on the bearing assembly and its operating conditions.

This scheme starts with an initial thermal input bend, θ_i. The overall "gain" vector, G, of the three transfer functions is defined as the ratio of the output bend, θ_o, and the input bend, θ_i. The rotor system is unstable when the real part of the complex vector, G, is greater than unity. Since a practical rotor usually has two overhung ends, the program establishes this gain vector, G, for each overhung end. When establishing the vector for one overhung end, of course the influence from the other overhung end also must be taken into account. Differential temperatures across a bearing journal were measured on a rotating shaft for various configurations of fluid-film bearings and different orbit sizes. These experimentally obtained bearing data are implemented to quantitatively describe the thermal effect, T(t, Ω).

The sequence of the program is as follows. Depending on the overhang geometry, the program first calculates the unbalance for unit bending at the bearing journals, respectively. Then, the rotor response at the bearing locations due to this unbalance, can be calculated using a general rotor response program. This can be done for a defined rotor speed range with small speed increments. From the calculated rotor response, which also includes phase information, the location of the hot spot of the shaft is established. The experimentally obtained data are implemented here to establish the differential temperature across the shaft. From this differential temperature, a resulting output thermal bend, θ_o, including its angular direction is calculated. The complex gain vector, G, results from the ratio between the output and the input bend. Figure C-1 shows a typical output plot of an example analysis that shows the real part of the gain vector, G, versus rotor speed. From this figure, it can be seen that the DE overhung end is not causing any trouble. However, at a speed of around 10,500 rpm, the rotor in this example becomes unstable, because of the NDE overhung end. For this rotor end, the real part of the complex gain vector, G, is exceeding unity. Above 13,800 rpm, the rotor becomes stable again, due to a phase change in the dynamic system.

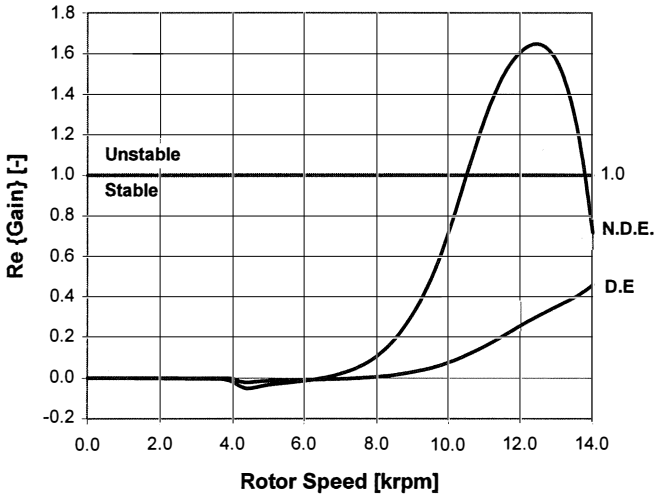

Figure C-1. Real Part of Gain Vector Versus Rotor Speed.

REFERENCES

ASME Power Test Codes, 1965, "Compressors and Exhausters," PTC 10.

American Petroleum Institute Standard, 1979, "Centrifugal Compressors for General Refinery Service," API 617, Fifth Edition.

American Petroleum Institute Standard, 1988, "Special-Purpose Gear Units for Refinery Service," API 613, Third Edition.

Corcoran, J. P., Rea, H., Cornejo, G. A., and Leonhard, M. L., 1997, "Discovering, the Hard Way, How a High Performance Coupling Influenced the Critical Speeds and the Bearing Loading of an Overhung Radial Compressor—A Case History," *Proceedings of the Twenty-Sixth Turbomachinery Symposium,* Turbomachinery Laboratory, Texas A&M University, College Station, Texas, pp. 67-78.

Faulkner, H. B., Strong, W. F., and Kirk, R. G., 1997, "Thermally Induced Synchronous Instability of a Radial Inflow Overhung Turbine PART II," Proceedings of ASME Design Engineering Technical Conference, Sacramento, California.

de Jongh, F. M. and Morton, P. G., 1996, "The Synchronous Instability of a Compressor Rotor Due to Bearing Journal Differential Heating," ASME Transactions, Journal of Engineering for Gas Turbines and Power, *118*, pp. 816-824.

Kellenberger, W., 1979, "Spiral Vibrations Due to Seal Rings in Turbogenerators. Thermally Induced Interaction Between Rotor and Stator," ASME Paper No. 79-DET-61.

Keogh, P. S. and Morton, P. G., 1993, "Journal Bearing Differential Heating Evaluation with Influence on Rotordynamic Behaviour," *Proceedings of the Royal Society*, London, England, *A441*, pp. 527-548.

Keogh, P. S. and Morton, P. G., 1994, "The Dynamic Nature of Rotor Thermal Bending Due to Unsteady Lubricant Shearing Within a Bearing," *Proceedings of the Royal Society*, London, England, *A445*, pp. 273-290.

Morton, P. G., 1994, "Recent Advances in the Study of Oil Lubricated Journal Bearings," *Proceedings of the Fourth International Conference on Rotor Dynamics,* IFFToMM, Chicago, Illinois, pp. 299-305.

Newkirk, B. L., 1926, "Shaft Rubbing," *Mechanical Engineering*, *48*, pp. 830-832.

Schmied, J., 1987, "Spiral Vibrations of Rotors," *Rotating Machinery Dynamics*, *2*, Proceedings of ASME Design Technology Conference, Boston, Massachusetts.

Stroh, C., MacKenzie, J., and Rebstock, J., 1996, "Options for Low Speed and Operating Speed Balancing of Rotating Equipment," *Proceedings of the Twenty-Fifth Turbomachinery Symposium,* Turbomachinery Laboratory, Texas A&M University, College Station, Texas, pp. 253-258.

ACKNOWLEDGEMENTS

The authors wish to thank the management of Demag Delaval Turbomachinery for their permission to publish this paper.